IEEE Photonics Journal
An IEEE Photonics Society Publication

Single LED Beacon-Based 3-D Indoor Positioning Using Off-the-Shelf Devices

Volume 8, Number 6, December 2016

Yinan Hou
Shilin Xiao
Meihua Bi
Yuankai Xue
Wansheng Pan
Weisheng Hu

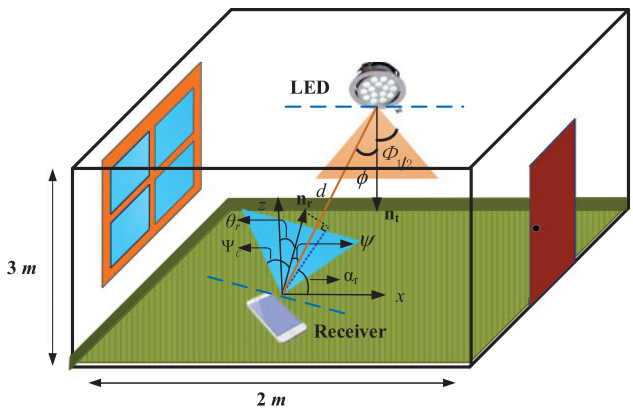

DOI: 10.1109/JPHOT.2016.2636021
1943-0655 © 2016 IEEE

IEEE photonics SOCIETY
IEEE

Single LED Beacon-Based 3-D Indoor Positioning Using Off-the-Shelf Devices

Yinan Hou,[1] Shilin Xiao,[1] Meihua Bi,[1,2] Yuankai Xue,[1] Wansheng Pan,[1] and Weisheng Hu[1]

[1]State Key Laboratory of Advanced Optical Communication Systems and Networks, Shanghai Jiao Tong University, Shanghai 200240, China
[2]College of Communication Engineering, Hangzhou Dianzi University, Hangzhou 310018, China

DOI:10.1109/JPHOT.2016.2636021

Manuscript received October 25, 2016; revised November 28, 2016; accepted December 1, 2016. Date of publication December 7, 2016; date of current version December 19, 2016. This work was supported in part by the National "863" Hi-tech Project of China under Grant 2013AA013602; in part by the National Nature Science Fund of China under Grant 61271216, Grant 61221001, and Grant 61501157; in part by the National "973" Project of China under Grant 2010CB328205, Grant 2010CB328204, and Grant 2012CB315602; and in part by the Natural Science Foundation of Zhejiang Province under Grant LQ16F050004. Corresponding author: Y. Hou (houyinan@sjtu.edu.cn).

Abstract: In this paper, we demonstrate a single light-emitting diode (LED) beacon-based 3-D indoor positioning scheme by experiment and theoretical derivation, which can overcome the limitation of multiple LED beacons involved in one positioning process. Only off-the-shelf devices are employed in this scheme, such as an image sensor, a gyroscope, and a photodiode, which have been integrated in most of commercial available smartphones so that it is compatible with most of mobile terminals. Moreover, with these simple devices, we estimate the 3-D position by using the received-signal-strength (RSS) and angle-of-arrival (AoA)-based hybrid positioning algorithm. The performance of this scheme is investigated in scenarios of the ceiling-mounted and the wall-mounted LED. The corresponding results show that, by using this scheme, 7.3 cm and 67.2 cm mean positioning errors are achieved in the ceiling and the wall LED cases, respectively. Therefore, this scheme may be considered as one of the competitive indoor positioning candidates in the future.

Index Terms: Visible light communication (VLC), indoor optical positioning, light-emiting diode (LED), smartphone.

1. Introduction

Recently, with the great demands for indoor location-based services, using the indoor positioning systems (IPSs) has been a subject of growing interest. The traditional global positioning system (GPS) [1], owing to its limited positioning accuracy, cannot be used in indoor settings. Meanwhile, due to the effect of multipath fading and non-line-of-sight (NLoS) conditions, the radio frequency (RF)-based IPS [2] is difficult to achieve the high-accurate positioning. However, the IPS based on visible light communication (VLC) [3]–[6], namely, the "light positioning system (LPS) [7]," has attracted great attention and is considered as one of the most attractive solutions for its special advantages of high positioning accuracy, no RF interference, etc. In [8], based on the received-signal-strength (RSS) from at least three ceiling-mounted LED beacons, a 3-D LPS with less than 0.4 m positioning errors is verified. In addition, the authors in [9] propose an LPS based on angle-of-arrival (AOA) algorithm with a corner-cube photo-receiver, which achieves 5 cm mean error with

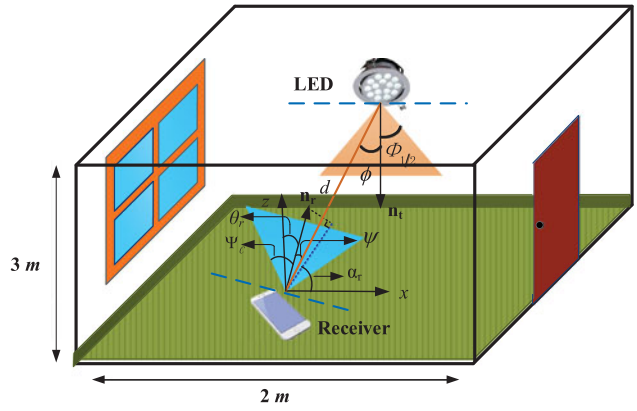

Fig. 1. Model of the proposed positioning scheme.

three ceiling-mounted LED beacons. In [10], a LPS based on a mobile camera is proposed, which achieve a decimeter-level accuracy with five ceiling-mounted LED beacons. However, in these LPSs, multiple LED beacons are necessary in one positioning process, which would make the LPSs disabled when the LED beacons are not enough.

To solve this problem, we introduce a novel single LED beacon-based 3-D indoor positioning scheme by employing only off-the-shelf devices (a PD, an image sensor, and a gyroscope), which have been integrated in most of commercial available smartphones. Based on this configuration, 3-D positioning can be achieved by using the RSS/AOA-based hybrid positioning algorithm within two application scenarios which are the ceiling-mounted and the wall-mounted LED (the LED could be mounted on the wall in some scenarios such as stairs, corridors, and so on). The performance of our scheme is investigated by experiment and the results show that 7.3 cm and 67.2 cm mean positioning errors are achieved in the ceiling and the wall LED cases respectively.

The contributions of this work can be specified as follows. First, we propose a novel single LED beacon-based LPS to overcome the problem of multiple LED beacons involved in one positioning process. Second, compared to the single LED beacon-based LPS [11], no complicated structure but only the off-the-shelf devices are utilized in this scheme. Moreover, these devices have been integrated in most of commercial available smartphones, which makes our scheme be easily compatible with most of mobile terminals. Third, unlike the image sensor-based LPS [10], image sensor in our scheme is only used to estimate the AOA bearing from the LED beacon not to demodulate the beacon signal. By reason of only signal frequency detection, only one image is required in one positioning process. Therefore, the image processing is relative simple. Finally, according to the location of the LED beacon mounted in practice, the performance in two scenarios of the ceiling-mounted and the wall-mounted LED are investigated by experiment.

2. Methodology

2.1. System Model

Fig. 1 illustrates the proposed scheme model. Here, the radiant intensity of a LED can be assumed to follow a Lambertian radiation pattern due to its large beam divergence [12]. The line-of-sight (LoS) channel gain can be given by [13]

$$H = \begin{cases} \dfrac{(m+1)A}{2\pi d^2}\cos^m(\phi)\cos(\psi)T_s(\psi)G(\psi), & 0 \le \psi < \Psi_C \\ 0, & \psi \ge \Psi_C, \end{cases} \tag{1}$$

where the parameters are as follows. m is the Lambertian order and defined as: $m = \frac{-ln2}{ln(cos(\Phi_{1/2}))}$, where $\Phi_{1/2}$ is the semi-angle at half illuminance of a LED. A is the area of an optical detector. d is the distance between a transmitter and a receiver. $T_s(\psi)$ is the gain of an optical filter, and $G(\psi)$ is the gain of an optical concentrator. ϕ is the irradiant angle, ψ is the incident angle, and Ψ_C is the field-of-view of the receiver.

The 3-D locations of the LED and the receiver are assume to be $\mathbf{l}_t = (x_t, y_t, z_t)^T$ and $\mathbf{l}_r = (x_r, y_r, z_r)^T$, respectively, and their normal vectors are denoted as $\mathbf{n}_t$ and $\mathbf{n}_r$, which can be defined as

$$\mathbf{n}_t = (\cos(\alpha_t)\sin(\theta_t), \sin(\alpha_t)\sin(\theta_t), \cos(\theta_t))^T \tag{2}$$

$$\mathbf{n}_r = (\cos(\alpha_r)\sin(\theta_r), \sin(\alpha_r)\sin(\theta_r), \cos(\theta_r))^T \tag{3}$$

where α_t and α_r are the azimuth angles of the LED and the receiver respectively, which are defined as the angles between the x-axis and the orthogonal projections of the normal vectors of the LED and the receiver to the xy-plane. θ_t and θ_r present the polar angles of the LED and the receiver respectively, which are defined as the angles between the z-axis and the normal vectors of the LED and the receiver. Moreover, α_t and θ_t are determined by the location of the LED while α_r and θ_r are determined by the measurements of a gyroscope in the receiver.

Meanwhile, the irradiant angle and the incident angle are given by [14]

$$\cos(\phi) = \mathbf{n}_t \cdot \frac{\mathbf{l}_r - \mathbf{l}_t}{d} \tag{4}$$

$$\cos(\psi) = \mathbf{n}_r \cdot \frac{\mathbf{l}_t - \mathbf{l}_r}{d}. \tag{5}$$

For the case of the ceiling LED, $\alpha_t = 0^\circ$ and $\theta_t = 180^\circ$, and therefore, $\cos(\phi) = (z_t - z_r)/d$, and for the case of the wall LED, if we assume LED's normal vector towards the positive direction of the y-axis of the room, $\alpha_t = 90^\circ$ and $\theta_t = 90^\circ$, so $\cos(\phi) = (y_t - y_r)/d$.

When the emitted optical power P_{ot} is received by the receiver, the incident optical power from LoS path P_{or} can be given by $P_{or} = P_{ot}H$, and the corresponding electrical power P_{er} is given by $P_{er} = R(\lambda P_{or})^2$, where R is the equivalent impedance of the receiver, and λ is the optical detector responsivity. In our system, there are no optical filter and concentrator, and therefore, we can get

$$P_{er} = \frac{c}{d^4}\cos^{2m}(\phi)\cos^2(\psi) \tag{6}$$

where c is a constant and defined as

$$c = \frac{R\lambda^2 {P_{ot}}^2 A^2 (m+1)^2}{4\pi^2}. \tag{7}$$

In practical system, the total incident optical power P_{total} contains the ambient light power P_{bg}, the incident optical power from LoS path P_{or} and NLoS path P_{NLoS}. In general, only P_{or} is used for positioning in LPS, while P_{NLoS} and P_{bg} are both viewed as noise power. The total noise variance can be given as

$$N = \sigma^2_{shot} + \sigma^2_{thermal} + R(\lambda P_{NLoS})^2 \tag{8}$$

where σ^2_{shot} is the shot noise variance which is depended on P_{total}, and $\sigma^2_{thermal}$ is the thermal noise variance which is depended on the receiver's parameters. σ^2_{shot}, $\sigma^2_{thermal}$, and P_{NLoS} are all described detailedly in [13]. The signal-to-noise (SNR) due to LoS path can be defined as

$$SNR = 10\log_{10}\left(\frac{P_{er}}{N}\right). \tag{9}$$

2.2. AOA Estimation

By using an image sensor and a gyroscope, the AOA bearing from the LED beacon can be estimated. Here, AOA involves the incident light azimuth angle α_p, which is defined as the angle

between the x-axis and the orthogonal projection of incident light to the xy-plane, and the incident light polar angle θ_p which presents the angle between the z-axis and incident light. In addition, two frames are used as reference, which are room frame of reference $(x, y, z)^T$ and receiver frame of reference $(x', y', z')^T$. If the room coordinates of the LED and the image sensor are presented as $(x_t, y_t, z_t)^T$ and $(x_{r1}, y_{r1}, z_{r1})^T$ respectively, and the receiver coordinates of the LED projection center on the image are $(x_l, y_l, z_l)^T$, we can get

$$(x_t, y_t, z_t)^T = \mathbf{R} \times k(x_l, y_l, z_l)^T + (x_{r1}, y_{r1}, z_{r1})^T. \tag{10}$$

Subsequently

$$(x_t - x_{r1}, y_t - y_{r1}, z_t - z_{r1})^T = \mathbf{R} \times k(x_l, y_l, z_l)^T, \tag{11}$$

where k is a scale factor of the receiver coordinates of the LED and its projection to the image. $\mathbf{R}$ is a 3×3 rotation matrix which is given by

$$\mathbf{R} = \begin{bmatrix} \cos(\rho) & \sin(\rho) & 0 \\ -\sin(\rho) & \cos(\rho) & 0 \\ 0 & 0 & 1 \end{bmatrix} \begin{bmatrix} \cos(\eta) & 0 & -\sin(\eta) \\ 0 & 1 & 0 \\ \sin(\eta) & 0 & \cos(\eta) \end{bmatrix} \begin{bmatrix} 1 & 0 & 0 \\ 0 & \cos(\delta) & \sin(\delta) \\ 0 & -\sin(\delta) & \cos(\delta) \end{bmatrix} \tag{12}$$

where δ, η, and ρ are the receiver's pitch angle, roll angle, and yaw angle which are all measured by a gyroscope in the receiver. From (12), the receiver's azimuth angle α_r and polar angle θ_r defined in (2) and (3) can be determined by

$$\begin{cases} \alpha_r = \tan^{-1}\left(\frac{\tan(\delta) + \sin(\eta)\tan(\rho)}{\tan(\delta)\tan(\rho) - \sin(\eta)}\right) \\ \theta_r = \cos^{-1}(\cos(\eta)\cos(\rho)). \end{cases} \tag{13}$$

Therefore, from the geometric relationship of the LED beacon and the image sensor, the azimuth angle α_p and the polar angle θ_p of the incident light can be defined as

$$\begin{cases} \alpha_p = \tan^{-1}\left(\frac{x_t - x_{r1}}{y_t - y_{r1}}\right) \\ \theta_p = \tan^{-1}\left(\frac{\sqrt{(x_t - x_{r1})^2 + (y_t - y_{r1})^2}}{(z_t - z_{r1})^2}\right). \end{cases} \tag{14}$$

Substituting (11) and (12) into (14), the angles α_p and θ_p can be estimated.

In addition, the coordinates of the LED projection center in the image can be determined by the following steps. Firstly, the image captured by the image sensor is grayed. Secondly, the image is filtered by a binary OTSU filter [15]. Lastly, the image is blurred and the LED projection center is determined by means of averaging all points in the projection of the LED beacon. Moreover, the gyroscope accuracy is also discussed. In general, the accuracy of the raw gyroscope outputs is quite low on account of its serious zero drift effect. However, after compensation and calibration, this effect can be suppressed effectively and the accuracy can be improved greatly. According to our experiment results, the maximum angle error measured by the gyroscope in iPhone 6 is about 2°. Besides, the distance between the lens and imager in the image sensor z_l is an important parameter, which is used to estimate the AOA bearing, and it would change with the distance between the object and lens, but fortunately, it deviates only 0.7% when the distance from the object to lens changes from 1 m to infinity [10]. Moreover, the distance between LED and receiver is only several meters, so it's reasonable to assume z_l to be a constant for positioning. Based on known locations of the LED beacon and the image sensor (the front facing camera of iPhone 6 is used in this paper), z_l is set with 1230 pixels.

2.3. RSS/AOA-Based Hybrid 3-D Positioning Algorithm

In addition, by using the RSS/AOA-based hybrid positioning algorithm, 3-D positioning can be achieved. The schematic of the positioning algorithm is illustrated in Fig. 2. Here, the coordinates of the LED and the receiver are still assumed to be $\mathbf{l}_t = (x_t, y_t, z_t)^T$ and $\mathbf{l}_r = (x_r, y_r, z_r)^T$, respectively

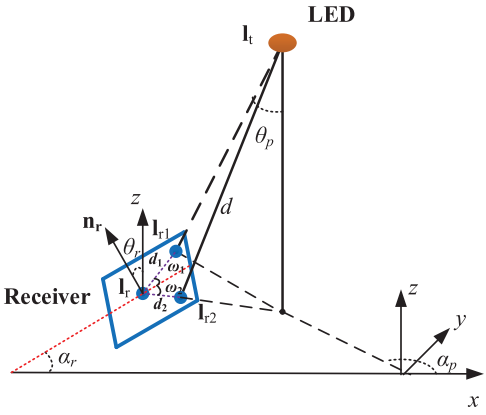

Fig. 2. Schematic of the RSS/AOA-based hybrid 3-D positioning algorithm.

which indicate their center coordinates. In the receiver, an image sensor and a PD are assumed to be deployed on the positions of $\mathbf{l}_{r1} = (x_{r1}, y_{r1}, z_{r1})^T$ and $\mathbf{l}_{r2} = (x_{r2}, y_{r2}, z_{r2})^T$. Although the image sensor and the PD can be deployed on any positions of the receiver, the relationships of their positions and the receiver center should be known in advance. As shown in Fig. 2, d_1 and d_2 are defined as the distances from the image sensor and the PD to the receiver center, ω_1 is the angle between the receiver's axis and the line through the receiver center as well the image sensor, and ω_2 is the angle between the receiver's axis and the line through the receiver center as well the PD, the relationships of $\mathbf{l}_{r1}$, $\mathbf{l}_{r2}$, and $\mathbf{l}_t$ can be given as

$$\begin{cases} \mathbf{l}_{r1} = \mathbf{l}_r + d_1(\cos(\alpha_r + \omega_1)\sin(\theta_r), \sin(\alpha_r + \omega_1)\sin(\theta_r), \cos(\theta_r))^T \\ \mathbf{l}_{r2} = \mathbf{l}_r + d_2(\cos(\alpha_r + \omega_2)\sin(\theta_r), \sin(\alpha_r + \omega_2)\sin(\theta_r), \cos(\theta_r))^T. \end{cases} \tag{15}$$

From the measured RSS on the position $\mathbf{l}_{r2}$, we can get

$$\begin{cases} P_{er} = \dfrac{c}{d^4}\cos^{2m}(\phi)\cos^2(\psi) \\ d = \sqrt{(x_{r2} - x_t)^2 + (y_{r2} - y_t)^2 + (z_{r2} - z_t)^2}. \end{cases} \tag{16}$$

Based on the estimated AOA bearing (the azimuth angle α_p and the polar angle θ_p, as shown in Fig. 2), we can get

$$\begin{cases} \tan(\alpha_p) = \frac{x_t - x_{r1}}{y_t - y_{r1}} \\ \tan(\theta_p) = \frac{\sqrt{(x_t - x_{r1})^2 + (y_t - y_{r1})^2}}{(z_t - z_{r1})^2}. \end{cases} \tag{17}$$

Moreover, the locations of the LED beacon and the image sensor follow as

$$\begin{cases} x_{r1} > x_t, y_{r1} > y_t, 0 < \alpha_p \leq \dfrac{\pi}{2} \\ x_{r1} < x_t, y_{r1} > y_t, \dfrac{\pi}{2} < \alpha_p \leq \pi \\ x_{r1} < x_t, y_{r1} < y_t, \pi < \alpha_p \leq \dfrac{3\pi}{2} \\ x_{r1} > x_t, y_{r1} < y_t, \dfrac{3\pi}{2} < \alpha_p \leq 2\pi. \end{cases} \tag{18}$$

Based on (15)–(18), the receiver's 3-D position coordinates can be estimated. Note that our scheme is not limited in the application of one LED beacon, and it still works in multiple LED beacons case. By using the RF carrier allocation technology [16], different LED projections in the image can be distinguished by means of the image sensor's rolling shutter effect [10] and the mixed

beacon signals from different LED beacons can be extracted, respectively, by using a PD, a fast fourier transform (FFT) module, and the corresponding filters in the receiver. Moreover, every LED beacon can determine one 3-D location of the receiver, thus the positioning can be achieved by an optimization process trying to minimize the linear mean square (LMS) error [8].

3. Experimental Setup and Results

In the following, we design an experiment for evaluating this scheme performance. We use a Cree Xlamp XM-L LED with the semi-angle at half illuminance of 62.5° ($m = 0.897$) to be mounted on the ceiling and the wall in a 1 m × 1 m × 3 m model (due to space symmetry, this model can be extended to be 2 m × 2 m × 3 m). As for transmitter, 200-kHz signals generated by a FPGA evaluation board (KC705), are used to modulate the LED and the driven current is injected by a bias-tee circuit. According to the reference [14], the transmitted signals should contain the LED's information of ID, 3-D location, orientation, emitted optical power, and Lambertian order. In practical system, these signals can be generated and managed by a control center. If a new LED with a different type is mounted or the location of one LED is changed, we just need to update the signal beacons in the control center. Moreover, owing to low data rate and simple demodulation, on-off keying (OOK) modulation is selected as modulation format. In the receiver, we assume 25 reference points to be evenly distributed on the xy-plane in the model. Around each point, a PD (Thorlabs PDA100A silicon photodetector with 100 mm^2 active area and 0.62 A/W peak response) and an image sensor (the front facing camera of iPhone 6) are deployed on the positions of $\mathbf{l}_{r1}$ ($\omega_1 = 0°$, $d_1 = 5$ cm) and $\mathbf{l}_{r2}$ ($\omega_2 = 180°$, $d_2 = 5$ cm), respectively. The iPhone 6 is horizontal to the xy-plane and its compass direction is always towards the negative direction of the y-axis (the positive direction of the x-axis is 243° from north while the compass direction of iPhone 6 is 152° from north). Therefore, we can determine the pitch angle, roll angle, and yaw angle to be 0°, 0°, and −91°. The optical signals are received by the PD and the corresponding RSS is measured by a RF spectrum analyzer (in practical system, RSS can be obtained by an FFT module in smartphone). Meanwhile, by using image processing and the gyroscope measurements, the AOA bearing can be estimated. At last, with all measurement results, the 3-D position of receiver is determined by using the RSS/AOA-based hybrid positioning algorithm.

Moreover, the influence of ambient light is tested in the daytime for evaluating its effect on positioning results. The PD is firstly deployed on the location below the LED with 2-m height. Then, the LED is lighted and the receiver output power is measured with about −47.2 dBm. Next, the LED is turned off, and about −80 dBm output power is obtained. From these results, we can get the influence of ambient light in our experiment is so slight that it can be neglected. Besides, the parameter c in (7) is also determined. In general, only the optical flux is given in the datasheet of a commercial available LED while its emitted optical power is not included. But the PD used in our experiment, is relative to its responsivity with unit of A/W rather than A/lux. Therefore, c cannot be directly obtained from the datasheet. To solve this problem, according to [8], we fix the vertical distance between the LED beacon and the receiver in the room center. The normal vectors of the LED and the receiver are parallel to each other. Finally, we move the receiver towards the positive direction of the x-axis and measure the received signal powers on different positions. Fitting the measurements with the function of $(c\cos(\phi)^{2(m+1)})/d^4$, we can get $c = 0.76 \times 10^{-4}$.

3.1. Performance of the AOA Estimation

The performance of the image sensor-based AOA estimation is investigated by experiment in the cases of the ceiling-mounted and the wall-mounted LED, respectively. In the following part of this paper, the projection center of the LED beacon on the xy-plane is assumed to be the origin of room frame. Moreover, the vertical distance between the LED beacon and the receiver is set to 2 m. The error distribution of the azimuth angle α_p is firstly depicted in Fig. 3. As shown in Fig. 3(a) (the case of the ceiling-mounted LED), a great error is found on the origin of coordinates. The reason is that, as the smartphone is just deployed on the position below the LED, due to the mismatch

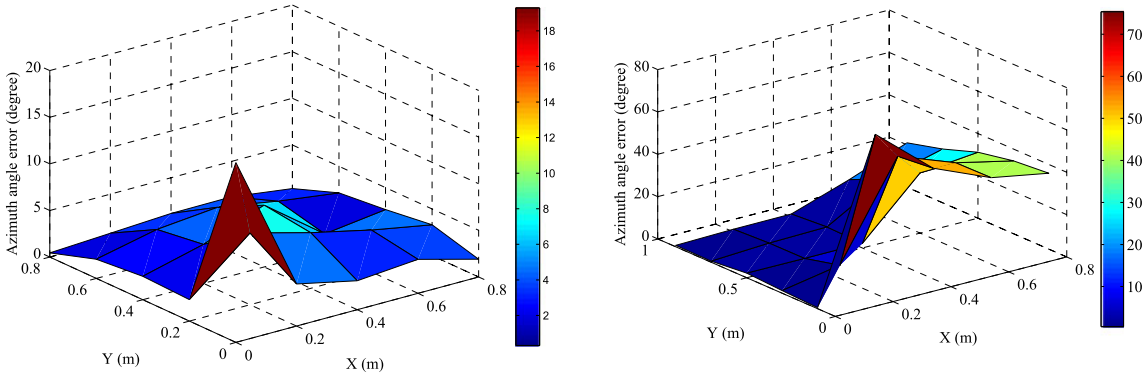

Fig. 3. Error distribution of the azimuth angle α_p in the cases of (a) the ceiling-mounted LED and (b) the wall-mounted LED.

TABLE 1
Polar Angle Errors in the Case of Ceiling-Mounted LED

y x	0 m	0.2 m	0.4 m	0.6 m	0.8 m
0 m	0.5°	0.7°	1.4°	1.7°	1.6°
0.2 m	0.5°	0.3°	0.9°	1.2°	1.2°
0.4 m	0.4°	0.5°	0.5°	0.7°	1.2°
0.6 m	0.4°	0.1°	0.4°	0.6°	1.2°
0.8 m	1.5°	1.5°	1.7°	2.1°	2.1°

between the real and assumed LED positions, a small center deviation of the LED projection in the image maybe induce a great estimation error of α_p. If the error on the origin is neglected, the mean error is only 3.1°. Moreover, as shown in Fig. 3(b) (the case of the wall-mounted LED), the greater errors are achieved on the positions near the *x*-axis (here, we still assume the LED's normal vector towards the positive direction of the *y*-axis). This is because as the smartphone gets close to the wall, the irradiant angle gets close to 90°, and therefore, the LoS light becomes weaker. Meanwhile, the NLoS light reflected by the ceiling gets stronger, which would affect the estimation of the LED projection center in the image dramatically so that the greater errors are found near the wall. This time, the mean error is 19.5°. The estimation error of the polar angle θ_p is also investigated and the results are shown in Tables I and II. As observed, when the LED beacon is mounted on the ceiling, the relative small estimation errors can be achieved, and only 0.9° mean error is achieved. However, when the LED beacon is mounted on the wall, the estimation errors become greater due to the influence of the NLoS light reflected by the ceiling. At this time, the mean error becomes 3.8°.

3.2. Performance of the Proposed Positioning Scheme

In this section, the performance in terms of positioning error is evaluated with the ceiling-mounted and the wall-mounted LED. Here, the positioning error is defined as the Euclidean distance between the estimated position and the real position. In our scheme, positioning error is mostly influenced by the AOA (α_p and θ_p) estimation error, the RSS measurement error, and the errors of the

TABLE 2
Polar Angle Errors in the Case of Wall-Mounted LED

y x	0 m	0.2 m	0.4 m	0.6 m	0.8 m
0.1 m	4.1°	2.6°	0.1°	1.8°	4.9°
0.3 m	1.1°	0.7°	5.1°	5.4°	7.1°
0.5 m	1.8°	0.3°	0.1°	7.9°	8.7°
0.7 m	0.6°	0.5°	0.2°	8.9°	10.5°
0.9 m	0.2°	0.3°	0.3°	9.4°	12.3°

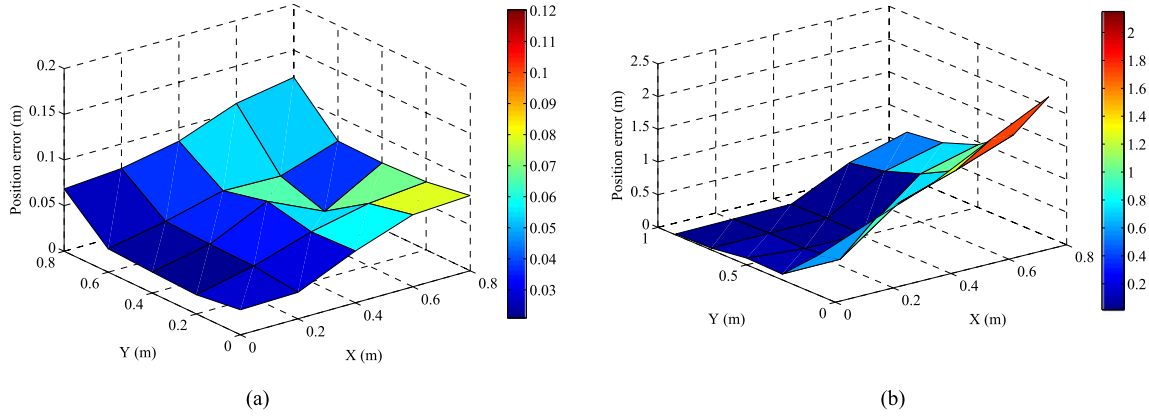

Fig. 4. Distribution of the positioning error induced by AOA in the cases of (a) the ceiling-mounted LED and (b) the wall-mounted LED.

receiver's azimuth angle α_r and polar angle θ_r. Because the errors of α_r and θ_r are irrelevant to the measurement positions, the impacts of the AOA and RSS on positioning error at different positions are investigated in the following. First, according to the real positions of the LED beacon and the receiver (the PD or the image sensor), the theoretical values of RSS and AOA can be easily obtained by using the estimation methods of RSS and AOA which are introduced in Section 2. Then, the theoretical RSS and the estimated AOA are substituted into the RSS/AOA-based hybrid positioning algorithm. The positioning error distribution is depicted in Fig. 4. From Fig. 4(a) (the case of the ceiling-mounted LED), 12 cm maximum positioning error and 2.1 cm minimum one are achieved on the positions of (0.8 m, 0.8 m) and (0 m, 0.2 m), respectively. The average positioning error is 5.8 cm. Moreover, compared to the results in Fig. 3(a), although a great estimations error of α_p is achieved on the origin of coordinates, the positioning error on this position is insensitive to the error of α_p. Contrastively, as observed in Fig. 4(b) (the case of the wall-mounted LED), 2.15 m maximum positioning error and 1.4 cm minimum one are achieved on the positions of (0.8 m, 0.1 m) and (0.2 m, 0.5 m) respectively. The average positioning error is 57.6 cm.

Furthermore, the positioning error induced by RSS is also investigated. Similarly, the theoretical AOA and the measured RSS are substituted into the hybrid positioning algorithm. By reason of RSS easily influenced by the NLoS light, we assume two applications in the case of the ceiling-mounted LED, which are the LED mounted on the center of ceiling (the room size is 4 m $\times$ 6 m $\times$ 3 m) and the LED mounted on the edge of ceiling (the LED is 1 m away from the wall). The positioning error results of the ceiling center-mounted LED is presented in Fig. 5(a). A 22 cm maximum positioning

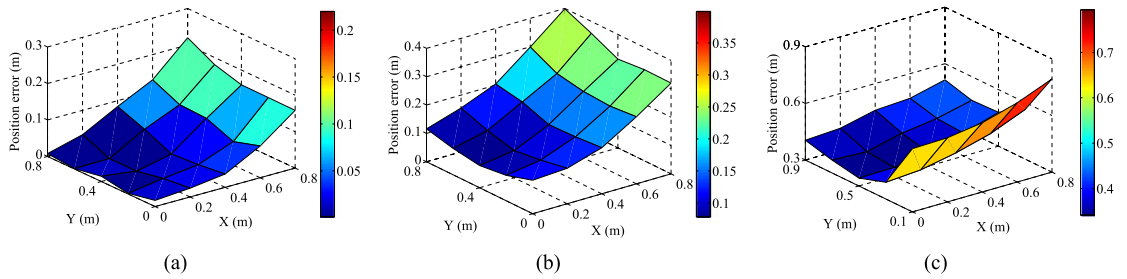

Fig. 5. Distribution of the positioning error induced by RSS in the cases of (a) the ceiling center-mounted LED, (b) the ceiling edge-mounted LED, and (c) the wall-mounted LED.

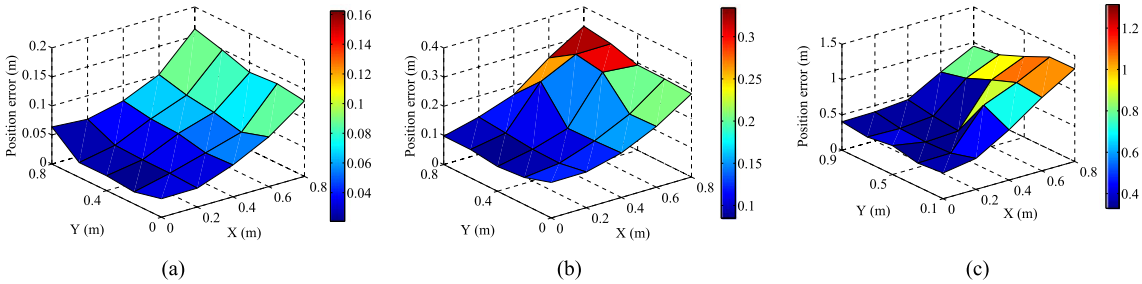

Fig. 6. Distribution of the overall positioning error in the cases of (a) the ceiling center-mounted LED, (b) the ceiling edge-mounted LED, and (c) the wall-mounted LED.

error and 0.1 cm minimum one are achieved on the positions of (0.8 m, 0.8 m) and (0 m, 0.6 m), respectively. The average positioning error is 6.8 cm. Besides, it is easily got that, the positioning errors on the *x*-axis are greater than the ones on the *y*-axis. These can be attributed to that, the position on the *x*-axis is nearer to the wall than the symmetrical position on the *y*-axis, which makes the receiver suffer from more influences of the NLoS light along the positive direction of the *x*-axis, hence achieving the greater positioning errors. Meanwhile, the positioning error results of the ceiling edge-mounted LED is presented in Fig. 5(c). Comparatively, 40 cm maximum positioning error and 7.9 cm minimum one are achieved on the positions of (0.8 m, 0.8 m) and (0 m, 0.4 m), respectively, while 19.5 cm average positioning error is achieved. In addition, the positioning error in the case of the wall-mounted LED is shown in Fig. 5(c). The LED's normal vector is still towards the positive direction of the *y*-axis, and the greater errors are found on the positions near the *x*-axis. These errors are not only contributed by the influence of the NLoS light but by the weak incident light strength as well.

The overall positioning error results are shown in Fig. 6. It is easily got that, when the LED is deployed in the center of ceiling, 16.2 cm maximum positioning error and 2.1 cm minimum one are achieved on the positions of (0.8 m, 0.8 m) and (0 m, 0.2 m) respectively, and 7.3 cm average positioning error is obtained. However, when the LED is mounted on the edge of ceiling, the maximum and minimum positioning error become 33.4 cm and 8.5 cm respectively, and the average error is 19.1 cm. That indicates the NLoS light would influence the scheme performance greatly, especially, when the receiver gets close to the wall. In addition, when the LED is mounted on the wall, the worst performance is achieved. As observed in Fig. 6(c), the average positioning error increases to 67.2 cm. Therefore, from the experimental results, we can find the performance with the ceiling-mounted LED is better than the one with the wall-mounted case. Moreover, due to the influence of the NLoS light, the performance at the edge of room is worse than the one in the center of room.

In the following, the impact of the receiver tilting on our scheme is discussed. This impact can be divided into two aspects. One is the impact on RSS estimation, and the other is the one on AOA

estimation. First, the former is discussed. Due to the receiver (the PD) tilting, the incident angle ψ in (1) is changed. That makes the channel model inaccurate, so great positioning errors are achieved. In order to improve the channel accuracy, the incident angle can be compensated based on the gyroscope measurements. Moreover, the high channel accuracy in the case of the PD tilting has been demonstrated [11], [12], [16]. Therefore, if the influence of the NLoS light is neglected, the receiver tilting would have little influence on RSS estimation. In addition, as for the impact on AOA estimation, the receiver tilting has little influence on the determination of the projection center of the LED beacon to the image. Meanwhile, the gyroscope accuracy has no selectivity to the receiver tilting angle. Therefore, the receiver tilting has also little influence on AOA estimation. Therefore, if the influence of the NLoS light is neglected, the performance in the case of the receiver tilting would be similar with the one in the case of the receiver horizontal.

At last, the complexity of our scheme is discussed. Due to the use of a PD, an image sensor, and a gyroscope in our receiver, the hardware complexity would be higher than other LPSs. However, our scheme is designed to be applied for smartphones and these devices have been integrated in most of commercial available smartphones, so the hardware complexity can be neglected. With respect to the software complexity, only one image captured by the image sensor in our scheme is necessary in one positioning process no matter how many the beacon signal is, and therefore, the image processing would be more simple than the image sensor-based LPS [10]. In addition, the power consumption can be reduced by combining with the inertial navigation system (INS). That is, our scheme only provide the target's original coordinates and calibration for INS.

4. Conclusion

In this paper, we propose a novel 3-D indoor positioning scheme using a single LED beacon to overcome the limitation of multiple LED beacons involved in one positioning process. In this scheme, only off-the-shelf devices are used, such as an image sensor, a gyroscope, and a PD, which have been integrated in most of commercial available smartphones, and therefore, our scheme can be compatible with most of mobile terminals. Based on the RSS/AOA-based hybrid positioning algorithm, 3-D positioning is achieved and the experiment investigates the scheme performance within the ceiling-mounted and the wall-mounted LED cases. The results show that our scheme can achieve 7.3 cm and 67.2 cm mean positioning errors in the ceiling and the wall LED cases, respectively.

References

[1] A. K. S. Wong, T. K. Woo, A. L. Lee, X. Xiao, V. H. Luk, and K. W. Cheng, "An AGPS-based elderly tracking system," in *Proc. 1st Int. Conf. Ubiquitous Future Netw.*, 2009, pp. 100–105.
[2] J. Xiong and K. Jamieson, "ArrayTrack: A fine-grained indoor location system," in *Proc. 10th USENIX Symp. Netw. Syst. Des. Implementation*, 2013, pp. 71–84.
[3] X. Huang, Z. Wang, J. Shi, Y. Wang, and N. Chi, "1.6 Gbit/s phosphorscent white LED based VLC transmission using a cascaded pre-equalization circuit and a differential outputs PIN receiver," *Opt. Exp.*, vol. 23, no. 17, pp. 22034–22042, 2015.
[4] N. Chi, M. Zhang, Y. Zhou, and J. Zhao, "3.375-Gb/s RGB-LED based WDM visible light communication system employing PAM-8 modulation with phase shifted Manchester coding," *Opt. Exp.*, vol. 24, no. 19, pp. 21663–21673, 2016.
[5] Z. Wang, C. Yu, W. Zhong, J. Chen, and W. Chen, "Performance of variable M-QAM OFDM visible light communication system with dimming control," in *Proc. 17th Conf. Opto-Electron. Commun.*, Jul. 2012, pp. 741–742.
[6] C. Chen, W. Zhong, and D. Wu, "Integration of variable-rate OWC with OFDM-PON for hybrid optical access based on adaptive envelop modulation," *Opt. Commun.*, vol. 381, pp. 10–17, 2016.
[7] S. Arnon, *Visible Light Communication.* Cambridge, U.K.: Cambridge Univ. Press, 2015, pp. 70–75.
[8] L. Li, P. Hu, C. Peng, G. Shen, and F. Zhao, "Epsilon: A visible light based positioning system," in *Proc. 11th USENIX Symp. Netw. Syst. Des. Implementation*, 2014, pp. 331–343.
[9] A. Arafa, S. Dalmiya, R. Klukas, and J. Holzman, "Angle-of-arrival reception for optical wireless location technology," *Opt. Exp.*, vol. 23, no. 6, pp. 7755–7766, 2015.
[10] Y. S. Kuo, P. Pannuto, K. J. Hsiao, and P. Dutta, "Luxapose: Indoor positioning with mobile phones and visible light," in *Proc. ACM Conf. Mobile Comput. Netw.*, 2014, pp. 447–458.

[11] S. Yang, H. Kim, Y. Son, and S. Han, "Three-dimensional visible light indoor localization using AOA and RSS with multiple optical receivers," *IEEE J. Lightw. Technol.*, vol. 32, no. 14, pp. 2480–2485, Jul. 2014.
[12] M. Yasir, S. W. Ho, and B. N. Vellambi, "Indoor positioning system using visible light and accelerometer," *IEEE J. Lightw. Technol.*, vol. 32, no. 19, pp. 3306–3316, Oct. 2014.
[13] T. Komine and M. Nakagawa, "Fundamental analysis for visible-light communication system using LED lights," *IEEE Trans. Consum. Electron.*, vol. 50, no. 1, pp. 100–107, Feb. 2004.
[14] G. B. Prince and T. D. C. Little, "A two phase hybrid RSS/AOA algorithm for indoor device localization using visible light," in *Proc. IEEE Conf. Glob. Commun.*, 2012, pp. 3347–3352.
[15] N. Otsu, "A threshold selection method from gray-level histograms," *IEEE Trans. Syst., Man, Cybern.*, vol. SMC-9, no. 1, pp. 62–66, Jan. 1979.
[16] H. Kim, D. Kim, S. Yang, Y. Son, and S. Han, "An indoor visible light communication positioning system using RF carrier allocation technique," *J. Lightw. Technol.*, vol. 31, no. 1, pp. 134–144, Jan. 2013.